

FINAL TECHNICAL REPORT

THE CRYSTALLIZATION AND CRYSTALLINE PROPERTIES OF
LARC-TPI

by

MICHAEL H. THEIL
Principal Investigator

with

PRAVIN D. GANGAL
Graduate Student

LANGLEY GRANT

* IN-76-CR

128391

P. 36

January 1, 1987 to December 31, 1988

College of Textiles
North Carolina State University
Raleigh, NC 27695-8301

NASA Grant NAG-1-723

(NASA-CR-191001) THE
CRYSTALLIZATION AND CRYSTALLINE
PROPERTIES OF LARC-TPI Final
Technical Report, 1 Jan. 1987 - 31
Dec. 1988 (North Carolina State
Univ.) 36 p

N93-13022

Unclas

G3/76 0128391

Table of Contents

| | |
|--------------------------------------------------------------------------------|----|
| ABSTRACT | 1 |
| I INTRODUCTION AND LITERATURE REVIEW..... | 2 |
| I.1 Synthesis of polyimides | 2 |
| I.2 Summary of properties and applications of aromatic polyimides | 3 |
| I.3 Crystallinity in Polymers | 4 |
| I.4 LARC-TPI, crystallization behavior and uses..... | 6 |
| I.4.a Crystallization behavior and research objectives..... | 6 |
| I.5 Characterization of LARC-TPI (Lot #72-501) | 6 |
| * II EXPERIMENTAL | 7 |
| II.1 Materials | 7 |
| II.2 Procedures | 7 |
| II.2.a Imidization experiments in m-cresol..... | 7 |
| II.2.b Fourier transform infrared spectrometry (FTIR) | 8 |
| II.2.c Thermogravimetric analysis (TGA) | 8 |
| II.2.d Differential scanning calorimetry (Dsc)..... | 8 |
| II.2.d.1 Dsc protocol involving annealing and subsequent melting | 8 |
| II.2.d.2 Crystallization kinetics and melting of samples so crystallized. | 9 |
| II.2.e X-ray diffraction..... | 9 |
| II.2.f Intrinsic viscosities | 9 |
| II.2.g Dissolution experiments..... | 10 |
| III RESULTS AND DISCUSSION | 10 |
| III.1 Infrared spectroscopy | 10 |
| III.2 Thermogravimetric analysis | 11 |
| III.3 Heating of LARC-TPI samples | 13 |
| III.4 Annealing experiments involving LM | 18 |
| III.5 Crystallization kinetics | 22 |
| III.6 X-ray diffraction | 27 |
| III.7 Dissolution experiments | 31 |
| IV Summary and conclusions..... | 32 |
| V REFERENCES | 33 |

ABSTRACT

LARC-TPI, a thermoplastic polyimide, has been studied in order to develop an understanding of its crystalline phase transition. Our experiments suggest that samples synthesized in different laboratories apparently had different degrees of imidization and their thermal behaviors differed accordingly. When the most crystalline of these polyimides was studied in some detail, we found that it melted irreversibly in that once a sample was completely melted it would not recrystallize. A polymer that did not recrystallize displayed a glass transition, which increased in temperature upon subsequent cooling and reheating. Solubility experiments indicated that heating above the crystalline melting temperature led to network formation in the polymer, a conclusion that is consistent with other behavior just mentioned. Differential calorimetric studies revealed that annealing at slow heating rates or under isothermal conditions resulted in dual melting transitions. These studies, supported by X-ray diffraction results, strongly indicate that the annealing process involves a solid-liquid-solid transformation. From an existing phenomenological model for the kinetics of phase transitions, kinetic parameters for these crystallizations have been evaluated. The Avrami exponents n increased with the annealing temperature in the protocol used in this study. Their values were about 2 or lower, thus indicating that crystallization may have followed a mechanism that included heterogeneous nucleation of a low dimensional order in which all the embryonic crystallites formed at the beginning of the process. A positive temperature coefficient for these crystallizations indicated that diffusion may have had a rate controlling influence and affected the values of n .

INTRODUCTION AND LITERATURE REVIEW

Linear aromatic polyimides are presently under consideration for both applications on future aircraft and spacecraft as matrix materials for composites and as non-conducting circuit board materials in electronic devices that operate under extreme service conditions. Their toughness and stability at high temperatures make them very attractive for these uses.

Polyimides are characterized by the presence of the phthalimide structure in the polymer backbone.¹

I.1 Synthesis of polyimides

Bogert and Renshaw performed the first reported synthesis of a polyimide.² They observed that when 4-aminophthalic anhydride or dimethyl-4-aminophthalate is heated, water or alcohol is evolved and a polyimide is formed. Edwards and Robinson were the first to describe the formation of a polyimide by the fusion of a diamine with a diester of a tetracarboxylic acid.³

A general method for the preparation of aromatic polyimides has been described by Edwards⁴ and by Endrey.⁵ It involves the synthesis of a soluble poly(amic acid), the precursor of the related polyimide. Polyamic acid preparation takes place in polar solvents such as N,N-dimethylacetamide and involves the direct reaction of dianhydride and diamine.

Polyamic acids can be converted to polyimides either by thermal dehydration or by chemical means. The thermal method has been described in various publications.⁶⁻¹⁰ Generally, it involves the partial drying of a solvated polyamic acid film and then gradual heating to the temperature of imidization. Thermal treatment at high temperatures (above 473.2 K) is generally performed in vacuum or in an inert atmosphere. Commonly, chemical conversion may use dehydrating agents such as acid anhydrides and catalysts such as tertiary amines. Aromatic polyimides are often extremely difficult to process due to their high melting points and their insolubility.¹¹

Usually, synthesis of polyimides involves formation of a soluble polyamic acid precursor that must be dissolved in a high-boiling solvent and later converted to the polyimide by heating to high temperature. This particular treatment causes evolution of water and residual solvent. The use of *meta*-substituted aromatic diamines in the preparation of linear polyimides has improved the processability of these polymers by lowering glass transition temperatures T_g from those polyimides prepared from the *para*-substituted diamines. The synthesis of such polymers is accomplished in a non-toxic, low-boiling ether solvent. Such measures have resulted in improving processability of polyimides while maintaining their useful properties.¹¹

A linear thermoplastic polyimide, "LARC-TPI," that incorporates many desirable characteristics such as suitability for a variety of high temperature applications, has been developed and characterized at NASA's Langley Research Center. LARC-TPI is produced when 3,3',4,4'-benzophenonetetracarboxylic acid dianhydride is reacted with 3,3'-diaminobenzophenone. It was first synthesized by Bell and coworkers^{11,12} who found that 1,2-dimethoxyethane (diglyme) was

an effective solvent for the polyamic acid that is a precursor to LARC-TPI.^{12,13} The method of synthesis involves the preparation of soluble precursor, a poly(amic acid) which is then converted to polyimide either by thermal or chemical imidization.

The laboratory scale, chemical imidization of the precursor polyamic acid for LARC-TPI being used at the Langley Research Center, NASA, by Dr. T. L. St. Clair is described here.¹⁴ Polyamic acid in reagent grade diglyme (15% concentration of solids by weight) is placed in a laboratory adaptation of a household blender. An equal volume of N-methyl-2-pyrrolidinone (NMP) is added to the blender, and the mixture is stirred for about a half h for homogeneity that is important for good imidization. To this mixture an equal volume of triethylamine (TEA) is added, and the whole mixture is stirred for about 15 min. Acetic anhydride is added to the blender in a volume equal to that of the polyamic acid solution, and the mixture is stirred for 12 h while the polymer precipitates. The polymer thus obtained is filtered and dried at 373.2 K for one h and then is heated at 423.2 K in a vacuum oven for about one h to complete the imidization.

I.2 Summary of properties and applications of aromatic polyimides

- Thermal properties Polyimides have excellent thermal stabilities¹⁵ and can be used at temperatures as high as 573.2 K.¹⁶ The thermal stabilities of polyimides depend on their backbone compositions.¹ The polymer loses heat resistance but usually becomes more soluble and processable as the imide functional group is diluted with less stable structures.
- Solvent and chemical resistance: Polyimides are generally inert to organic solvents and oils and are not affected by dilute acids.
- Color: Polyimides are intense yellow to red in color, which is related to the structure of the diamine component.⁸
- Crystallinity: Aromatic polyimides from diamines such as *p*-phenylenediamine crystallize spontaneously upon preparation.⁸ Other observations of crystallinity of polyimides are to be found in the literature.^{10,17}
- Applications: Polyimides are used as varnishes, neat resins, films (Kapton, Skybond-700), flameproof foams and matrix materials for reinforced composites having excellent properties at high temperatures. They also show great usefulness and versatility as adhesives.^{1,12,16} It can bond metals such as titanium, aluminum, stainless steel, etc. LARC-TPI can also be used to bond large pieces of polyimide film to produce flexible, 100% void-free laminates for flexible circuit applications and it has been used as an adhesive for bonding ultra thin polyimide film in the NASA-Solar Sail Program.^{16,18} It is its superior adhesive potential that makes it suitable for large area bonding of a graphite reinforced composite material.^{11,12,16,18} Although thermosetting resins are generally used as matrices for composites, crystalline thermoplastic polymers do offer an attractive alternative. Thermoplastics are generally polymerized prior to their use as a matrix material, which, in

contrast to thermosets gives them very good shelf life. Unlike thermosets which cross-link upon melting, recrystallizable thermoplastics can be repaired through reheating. LARC-TPI was also a candidate for the large-area bonding of an experimental graphite composite wing panel in the NASA-Supersonic Cruise Research Program.¹⁶

I.3 Crystallinity in Polymers

Polymers, as long chain molecules of diverse flexibilities, can exist in the amorphous state, in various liquid crystalline states, or in the crystalline state. However, the attainment of an appreciable degree of crystallinity is dependent on the presence of sufficient regularity along the chain and appropriate thermal and environmental circumstances.¹⁹⁻²¹ The amorphous state is characterized by configurational disorder of individual chains and of the overall system. In the crystalline state, individual chains are ordered. Collectively, chain molecules in crystallites are arrayed in a high degree of three-dimensional order and are usually aligned parallel to one another. The crystallites can give rise to X-ray and electron diffraction patterns that are like those produced by low molecular weight crystalline substances. However, in the case of synthetic polymers, the diffraction patterns suffer lack of detail and resolution due to typical crystallite thicknesses that are in the tens of nm and possible crystallite imperfections. The crystallites thus described undergo melting when heated, and their melting temperatures depend upon the molecular characteristics of the polymer as well as the habit of the crystallites. The latter characteristic in turn, is very sensitive to the thermal and other environmental history of the polymer during the crystallization process. The benchmark equilibrium melting temperature of an infinitely long, perfectly regular polymer chain may be written as T_m^0 and is defined by the equation

$$T_m^0 = \frac{\Delta H_u}{\Delta S_u} \quad (1)$$

where ΔH_u and ΔS_u are respectively the enthalpy of fusion and the entropy of fusion per mole of crystalline structural units of the polymer chain crystallized in its most stable form. The equilibrium melting temperature of a collection of polymer molecules having limitations in their chain lengths and in their molecular regularities may be designated as T_m . Besides the enthalpy and entropy parameters just given, an equation for this equilibrium melting temperature would include terms that reflect the finite crystallite size and attendant interfacial free energies imposed upon the system by these molecular limitations. In addition, we may define here the melting temperature of a crystal formed under non-equilibrium conditions, such as at undercoolings from the equilibrium melting temperature. This melting temperature, which may be designated as $T_{m(obs)}$, may be depressed from the previous one due to further constraints imposed upon its crystalline habit and the introduction of

imperfections due to the kinetic restraints of crystallization under non-equilibrium conditions.

The process of crystallization begins with nucleation and is continued by the growth of the nucleus to form the mature crystallite. Nucleation can occur by homogeneous or heterogeneous mechanisms. Homogeneous nucleation is characterized by the spontaneous aggregation of polymer chains below the melting point occurring randomly in space and randomly with respect to time. The exponent of time n in the phenomenological equation that describes the rate of phase transformation in which the new phase is developing from specific centers is called the Avrami exponent. Originating from specific centers, the transformation process, is by definition, nucleation controlled. The Avrami exponent is the combined function of the growth dimensions of a crystallite and its time dimension. The equation that describes this transformation is given as

$$\frac{X_c(t)}{X_c(\infty)} = 1 - \exp(-k' t^n) \quad (2)$$

in which $X_c(t)$ is the fraction of polymer that crystallizes at time t , $X_c(\infty)$ is the fraction of material that is ultimately crystallizable under the conditions of the experiment, and k' is a modified rate constant that takes into account that not all of the mass of a crystallizable polymer will ultimately crystallize. A conventional mechanistic interpretation of the values of Avrami exponents is given in Table I.1.²¹ Clearly, other possibilities exist, such as diffusion controlled heterogeneous nucleation, and crystallizations in which nucleation occurs at non-random times but not at the beginning of the process.²²

Table I.1 Avrami exponents

| Growth habit | Homogeneous nucleation | | Heterogeneous nucleation |
|-------------------|------------------------|-----------------------------|--------------------------|
| | Linear growth | Diffusion controlled growth | Linear growth |
| Three-dimensional | 4 | 2.5 | $3 \leq n \leq 4$ |
| Two-dimensional | 3 | 2 | $2 \leq n \leq 3$ |
| One-dimensional | 2 | 1.5 | $1 \leq n \leq 2$ |

I.4 LARC-TPI, crystallization behavior and uses

I.4.a Crystallization behavior and research objectives

Originally LARC-TPI was thought to be non-crystallizable. However, Burks, Hou, and St. Clair have reported that Mitsui Toatsu of Japan, a licensee of NASA's patents concerning the synthesis and the applications technology of LARC-TPI, has provided the Polymeric Materials Branch at NASA's Langley Research Center (LaRC) with a crystalline sample of that polymer.²³ The polymer can be melted at temperatures that are slightly above its glass transition temperature T_g . Upon melting, the polymer undergoes a remarkable decrease in viscosity to levels that should lead to improvements in polymer processability and thus to a wider range of applications for LARC-TPI. However, the low viscosity obtained upon heating to melting is transient for melts that are held at temperatures in the vicinity of the experimental melting temperature $T_{m(obs)}$ of the as-received sample (received at NASA).²³

At temperatures equal to or less than 493.2 K the complex viscosity increases in about 15 min. At 503.2 K and higher the viscosity increases at a much slower rate. Other rheological evidence and calorimetric evidence help to explain this phenomenon as one in which heating the partially crystalline polymer to between 543.2 K and 593.2 K causes existing crystallites to melt. The polymer, when held isothermally at the temperature at which it melted, will recrystallize to a thermodynamically more stable crystalline form.²³ The increased thermal stability of the recrystallized material may be due in part to nucleation induced morphological changes, *i.e.*, changes in crystalline habit due to higher crystallization temperatures. Changes in crystal structure, *i.e.*, polymorphism, with increasing crystallization temperatures have also been reported.²⁴

The findings discussed so far suggest new opportunities for the application of LARC-TPI. The existence of crystallinity would ensure better mechanical properties than those of amorphous polymers. The main objective of this research is to characterize phenomena associated with the crystallization of LARC-TPI and to develop an understanding of its crystallization behavior. Thus a basis will be established for making rational decisions with regard to its processing and applications.

I.5 Characterization of LARC-TPI (Lot #72-501)

Thermal properties of this specific lot have been studied by T. H. Hou and J. M. Bai.²³ Crystallization kinetics parameters that they determined are given in Table I.2. They observed that, in contrast to some other crystallizable thermoplastic resins, as received crystalline LARC-TPI powder is not readily crystallizable at temperatures above its initial melting point of 272°C. A semi-crystalline polymer can be obtained from the material annealed at temperatures below 320°C. Both $T_{m(obs)}$ and T_g increased upon annealing, thus indicating changes in both crystalline and amorphous regions. It has been suggested that

the change in amorphous region could be due to increase in molecular weight by a chain extension reaction. A purely amorphous structure resulted from the samples annealed at temperatures above 320°C. The Avrami exponent constants n , which are indicative of crystallization mechanism,^{20,21} were independent of annealing temperature.

Table I.2 Avrami exponents of LARC-TPI (Lot # 72-501)²³

| Annealing Temperature (K) | n |
|---------------------------|-------|
| 553.2 | 1.033 |
| 573.2 | 1.101 |
| 593.2 | 1.109 |

II EXPERIMENTAL

II.1 Materials

Three versions of LARC-TPI in powder form have been used in this study. One was prepared at NASA's Langley Research Center by the method described in section I.1. The Mitsui Toatsu Company of Japan prepared the second sample, which was identified by their Lot # 92-712. The imidization conditions for that sample are unknown to us. We prepared the third version in a homogenous system as described in section II.2.a. LARC-TPI polyamic acid precursors, one in *N,N*-dimethylacetamide (DMAC) and one in diglyme, were supplied by Dr. T. L. St. Clair of NASA's Langley Research Center. We designated these three samples LST, LM and LNC respectively.

II.2 Procedures

II.2.a Imidization experiments in *m*-cresol

We conjectured that a homogeneous system would be advantageous in efforts to obtain improvements in the degree of imidization obtained from the polyamic acid precursor of LARC-TPI. Because *m*-cresol is a solvent for LARC-TPI, it was used as a solvent in the imidization process.

One part of polyamic acid (15% solids by weight) in DMAC was added to *m*-cresol per 10 parts *m*-cresol by volume. The suspension thus obtained was kept overnight to allow the polyamic acid to dissolve in *m*-cresol. The solution was stirred for a few min in a household blender. Then a volume of TEA equal to that of the polyamic acid/DMAC suspension was added to it. Stirring was continued for 15 min and a like volume of acetic anhydride was added with continued stirring. The precipitated polymer was separated by filtration and washed with methanol.

II.2.b Fourier transform infrared spectrometry (FTIR)

A FTIR spectrophotometer manufactured by Beckman Instruments, equipped with an interactive light pen, and integrated plotter and disk drive accessory was used in this particular study. Nitrogen was used as a purge gas. The polymers, in powdered form, were formed into KBr pellets with Fisher Scientific IR grade potassium bromide. Spectra were obtained from the pellets thus prepared and from the same pellets after they were heated under vacuum at 150 °C for 14 h.

II.2.c Thermogravimetric analysis (TGA)

TGA experiments were carried out using a Perkin Elmer TGA 7 instrument. The polymer samples used were in powder form, and their masses were between 4.2 mg and 6.2 mg. All the experiments were performed in a nitrogen atmosphere. The sample pan used to hold the polymer powder was cleaned by heating it with a propane burner before starting a new experiment. Standard procedures, as described by the instrument manufacturer, were followed. The derivatives of the data with respect to temperature or time assisted in determining the onset, the peak, and end of the weight loss of the specimen.

II.2.d Differential scanning calorimetry (Dsc)

Both the Perkin Elmer DSC-2 and the DSC-7 Differential Scanning Calorimeter (DSC) models were used in this study for measurement of the thermal properties of the polymers such as melting, glass transition, and crystallization.

Samples of the polymer powder were weighed into aluminum sample pans on a Mettler analytical balance to a precision of 1.0×10^{-4} g. They were sealed in pans by use of a volatile sample sealer accessory. The masses of the samples used were between 3.0×10^{-4} g to 5.0×10^{-4} g. Each DSC instrument was calibrated for baseline optimization before each session of measurements. Indium and lead standards were used in calibrating the instruments with respect to temperature and enthalpy.

In early experiments, polymer samples were heated from 380.0 K through 630.0 K.

II.2.d.1 Dsc protocol involving annealing and subsequent melting

We did experiments involving isothermal annealing of LARC-TPI powder at selected temperatures and times, followed by controlled cooling and heating. The temperatures ranged from 450.0 K (176.8 °C) to 575.0 K (301.8 °C) and the times ranged from 0 min to 30 min. In these experiments, the specimens were taken to the desired annealing temperature, held for the selected time period, and then cooled to the startup temperature. The annealing temperatures chosen for such experiments were selected in accordance with initially observed melting temperatures during prior scanning of LM at 5° min^{-1} . Immediately following annealing, a treated specimen was heated at a scanning rate of 5° min^{-1} through melting.

II.2.d.2 Crystallization kinetics and melting of samples so crystallized.

We conducted general crystallization kinetics studies with the DSC-7. Of interest was the development of crystallinity during the isothermal hold periods. These crystallization temperatures were approached at scanning rates of $5^{\circ} \text{ min}^{-1}$ and $20^{\circ} \text{ min}^{-1}$ by programming the instrument. The initial melting temperature obtained when scanning a sample run at $5^{\circ} \text{ min}^{-1}$ was taken as a reference temperature for selecting a temperature for an isothermal hold. The duration for a given isothermal hold was selected so that a crystallization had effectively ceased at the end of that time period.

In a given isothermal kinetics study, certain preliminaries were observed. The instrument was first stabilized by holding the sample chamber at 303.2 K (30.0° C) for 3.00 min. The sample was heated to 513.2 K (240.0° C) at $30^{\circ} \text{ min}^{-1}$. From this temperature, the sample was heated at $5^{\circ} \text{ min}^{-1}$ or at $20^{\circ} \text{ min}^{-1}$ depending on the experiment. The isothermal study temperature ranged from 558.2 K (285.0° C) to 573.2 K (300.0° C), and a 60 min holding period was eventually deemed sufficient. The thermal data obtained during the hold period was used to study the crystallization kinetics of the polymer. Data were plotted as power evolved versus time. The peak program in the software library of the DSC-7 data station was used to calculate the cumulative energy evolved at intermediate points of a crystallization process by integrating over selected partial area intervals of the crystallization exotherm.

After the isothermal hold period, a sample was heated to 673.2 K (400° C) at the selected rate in order to determine the melting behavior of the crystallites formed during the isothermal hold period. We found that the quality of the baseline of the data was often compromised when data collection was continued over the entire extent of an experiment, namely heating followed by isothermal holding and the final heating. In those cases the experiments were rerun on new samples and data were collected only during the final heating stage. Both $T_{m(\text{obs})}$ and enthalpies of fusion were obtained from these procedures.

II.2.e X-ray diffraction

Wide angle X-ray diffraction patterns were collected from the three LARC-TPI samples as initially received or prepared as well as from some heat treated samples. Heat treatments were conducted in an oven under nitrogen, and a calibrated thermometer was used in monitoring the oven temperature. The powder specimens were held in proper position in a sample holder with clear adhesive coated tape. A Siemens diffractometer, equipped with a camera and using monochromatic copper $K\alpha$ X-rays of $\lambda = 1.542 \times 10^{-1} \text{ nm}$ (1.542 \AA) was used to take powder diffraction patterns.

II.2.f Intrinsic viscosities

Dilute solution, capillary viscometry measurements of series of concentrations of given polymer samples were conducted with Cannon-Fenske capillary viscometers. Measurements were made with the viscometers in a thermostatically controlled bath set at $303.15 \pm 0.02 \text{ K}$ ($30.00 \pm 0.02^{\circ} \text{ C}$). Under these

conditions, the efflux time for *m*-cresol, the solvent used in these characterizations, was 852.9 s in one viscometer and 2447.7 s in the other. The intrinsic viscosities of the as received LM and LST polymers were 0.040 and 0.032 respectively. Insufficient LNC was available for an intrinsic viscosity determination on that sample.

II.2.g Dissolution experiments

In order to study whether thermal treatments limited polymer solubility, we conducted dissolution studies of untreated and heat treated samples of LARC-TPI. The samples were heated as stated in Table III.13 and allowed to cool immediately thereafter. Several mg of each sample were placed in a separated 2.0 mL of portion of *m*-cresol. After 15 min at 333.2 K, each sample was visually inspected for dissolution.

III RESULTS AND DISCUSSION

III.1 Infrared spectroscopy

This study deals with the effects of heat treatment on the characteristics of LARC-TPI and specifically focuses on crystallinity. However, other characteristics may be affected by heat, and they may, in turn, affect crystallinity. We examined the untreated and some treated samples in order to qualitatively assess the effects of heating on imidization.

Table III.1 comparatively describes the presence of functional groups in the untreated samples and their counterpart heat treated samples. It lists the treatment given to the specimens and descriptions of the characteristic absorption bands due to the presence of amic acid and imide functional groups.

Table III.1 Infrared Characteristics of Untreated and Heat Treated LARC-TPI Polymers

| Sample description | Type of Treatment | Wave number cm ⁻¹ | | |
|--------------------|--------------------------------------|---------------------------------|-------------|-----------------------|
| | | 1547 | 1370 | |
| | | Qualitative | Qualitative | Normalized absorbance |
| LM | untreated | A | P | 1.00 |
| LNC | untreated | P | P | 1.00 |
| LST | untreated | A | P | 1.00 |
| LM | heated in vacuum at 423.2 K for 14 h | NC | NC | 1.02* |
| LNC | heated in vacuum at 423.2 K for 14 h | R | I | 1.57* |
| LST | heated in vacuum at 423.2 K for 14 h | NC | I | 1.77* |

P: present, A: absent, I: increase in absorbance, R: reduction in absorbance, NC: no significant change

*Ratios of heated to unheated absorbances.

In this study the absorption bands at 1370 cm^{-1} and at 1547 cm^{-1} are of significance. The former band is due to the tertiary nitrogen of the polyimide and is present in all cases; the latter band is attributable to the amide group N-H. We see this peak in the LNC sample, the one in which the imidization reaction was conducted in *m*-cresol. We observed the normalized absorbance at 1370 cm^{-1} in each polymer version to increase after heat treatment, indicating an increase in imide content, although it was small in the case of LM. The absorbance of the LNC sample at 1547 cm^{-1} decreased upon heating, showing a lessening of its amic acid content. We did not see significant changes for this absorption band in the thermally treated samples of the other two polymers. Yet, in the case of LST, the absorbance at 1370 cm^{-1} is increasing at the same time. If the source of the increase of imide groups in the LST polymer stems directly from an isoimide intermediate being converted to an imide, this effect would be explained.¹⁰ Indeed the infrared spectra of the virgin LM and LST show significant isoimide absorption peaks at 915 cm^{-1} , 1710 cm^{-1} and 1805 cm^{-1} in comparison with the aromatic stretching peak at 1015 cm^{-1} . Such is not the case for the LNC polymer. These results suggest that the imidization conducted in *m*-cresol was inefficient. Thus a higher amic acid group concentration was available for further reaction in LNC than in the other two polymers. This potential for reaction was then reflected in the results. In the cases of LM and LST, reaction of isoimide groups seems to have made more significant contributions to the increases in imide content than was the case for LNC.

III.2 Thermogravimetric analysis

Initially untreated LST and LM samples were used in this particular study. Infrared analysis as described in section III.1 indicates incomplete imidization of LARC-TPI and there has also been an indication that the relative degree of imidization goes to a higher level after the heat treatment. An incompletely imidized polymer would have a more irregular structure than one that is more completely imidized. Its structure would be essentially copolymeric. Such polymer chains crystallize less readily and form less stable crystallites than do regular chains. Chemical reactions occurring concomitantly with heating would also affect crystallization. We carried out isothermal crystallization kinetics studies at temperatures ranging from 558.2 K to 573.2 K . So it was necessary to check for occurrence of any mass loss during the normal scan as well as during the isothermal hold period of the sample that would be indicative of chemical reactions that occurred upon heating. These considerations prompted the design of experiments for a TGA study.

Table III.2 summarizes the important features TGA thermograms obtained for samples LM and LST. Trials 1 and 2 were conducted on the one sample of

Table III.2 Thermogravimetric analysis of LARC-TPI Samples LM and LST

| Trial | Polymer origin | Type of Treatment | Mass Change % | Onset* K or min | Peak* K or min |
|-------|----------------|----------------------------------------------------------------------------------------------------------------------------------------------------------------|---------------|-------------------------------------------------------------------------|-------------------------------------------------------------------------|
| 1 | LM | 308.2 K to 673.2 K at 5° min ⁻¹ | -3.2 | 429.1 | 458.8 |
| 2 | LM | 308.2 K to 673.2 K at 5° min ⁻¹ , rerun of sample used in of trial 1 | 0.0 | - | - |
| 3 | LM | 308.2 K to 773.2 K at 20° min ⁻¹ | -3.6 | ‡455.1; 671.9 | ‡481.6; 699.9 |
| 4 | LST | 308.2 K to 673.2 K at 5° min ⁻¹ | -7.6 | 397.1 | 501.1 |
| 5 | LST | 308.2 K to 673.2 K at 5° min ⁻¹ , rerun of sample used in trial 3 | -0.6 | not detectable | not detectable |
| 6 | LM | Ambient to 513.2 K, 30° min ⁻¹ ; (513.2-568.2 K), 5° min ⁻¹ ; isothermal hold at 568.2 K for 40 min; 568.2-713.2 K, 5° min ⁻¹ | -7.4 | ‡5.6 min after 5° per min heating begins* (541.4 K); 70.0 min (663.2 K) | ‡9.2 min after 5° per min heating begins* (559.2 K); 79.0 min (708.2 K) |

*A portion of trial 6 was conducted isothermally and data were recorded as a function of time.
‡Trials 3 and 6 showed two separate mass loss episodes as it was heated.

LM, and trials 4 and 5 involved the same sample of LST. Thus, trial 2 involved a reheating of LM according to the same schedule in which previously untreated LM was heated in trial 1. A similar statement applies to trials 4 and 5. There is a mass loss during first thermal treatment due to the evolution of volatile substances, but a repetition of that treatment produces no such effect. The fact that the second heating of each pair essentially yields no further mass loss seems to rule out polymer decomposition as the causal phenomenon. We may then expect that the volatile products are the condensation byproducts of amic acid imidization or residual solvents that are being evolved upon heating. The fact that infrared spectroscopy indicates that imidization progresses with heating suggests that the former alternative is at least partially responsible for the mass loss on the first heating. The LM sample lost less mass than the LST on the first heating. This could indicate that prior to thermal treatment, the residual amic acid group concentration in the virgin LM sample was lower than in the untreated LST sample. Yet the evolution of residual solvent could still contribute to the weight loss.

Heating the LM polyimide to a yet a higher temperature as in trial 3 results in a two stage evolution of volatile substances even though the heating process is

faster in this case than in trials 1 and 2. We can surmise that the first release of volatile substances for trial 3 is similar in nature to that which occurred in trial 1. Continued heating above approximately 672 K leads to additional mass loss that reaches its highest rate at approximately 700 K. Trial 6 involved a complex heating protocol. Our intention was to see if holding the polymer at a temperature below 673 K would lead to additional mass loss that we otherwise would have seen at temperatures above 673 K as in trial 3. The 7.6% mass loss was the highest that we saw for an LM sample. About 0.3 of the 7.6% mass loss took place at temperatures above 663 K. Thus, two disparately programmed experiments show a two stage mass loss for the LM polyimide. The first stage for trial 6 occurred at a higher temperature than observed for trial 3. During their early stages, trial 6 employed a faster heating rate than trial 3, thus reinforcing the idea that the mass loss seen is due to the evolution of imidization byproducts such as water. We would expect the imidization reaction to be dependent on reaction rates, and fast heating might move its expression to a higher temperature. On the other hand, solvent volatilization for such a small sample, should be quick and thus independent of temperature. The second stage of the mass loss occurred at approximately the same temperature in both instances. Heating in both trials had progressed at $5^{\circ} \text{ min}^{-1}$ for quite some time before the vicinity of 663 K was reached. Since imidization has occurred at the lower temperature, we are left with polymer degradation as one of the few remaining explanations for the mass loss at higher temperatures.

III.3 Heating of LARC-TPI samples

The thermal history of LARC-TPI determines its subsequent response to heating. It has been found that the once it was melted, LARC-TPI could not be recrystallized.¹⁵ We confirmed these findings.

Figure 1 shows Dsc thermograms for the untreated LNC, LST, and LM samples when heated at $20^{\circ} \text{ min}^{-1}$. Each of these polymers displays a single endotherm that is interpretable as being characteristic of fusion. The results of these experiments are summarized in the three examples of Table III.3. As found previously, recrystallization did not appear to occur since fusion endotherms were absent after cooling followed by reheating. Figure 2 shows three heating thermograms for LM as scanned at $20^{\circ} \text{ min}^{-1}$. The scans were performed on the same sample in a sequence that starts with the bottom thermogram. That thermogram is the same as that shown for LM in Figure 1. The thermogram immediately above it, obtained from the sample that displayed the endotherm after first cooling it, shows no fusion endotherm, but it displays a change in heat capacity (C_p) characteristic of a T_g . As shown in the second section of Table III.4, that T_g is lower than the $T_{m(\text{obs})}$. When the cooling-heating cycle was repeated yet another time on the same LM sample a T_g was seen again, but at a higher temperature than before.

Figure 3 shows that the scanning rate determined the characteristics of the fusion process. The lower curve is again the same scan that was shown for LM in

Figure 1. It was obtained at $20^\circ \text{ min}^{-1}$ and shows only one endotherm. At a slower scan

Table III.3 Thermal treatments of LARC-TPI samples

| Reference to Figure(s) | Sample and run no. | Thermal treatments | $T_{m(\text{obs})}$ or T_g (K) | Comments |
|------------------------|--------------------|-----------------------------------------------------------------------------------------------------------|----------------------------------|--------------------|
| 1-3 | LM-1 | heated at $20^\circ \text{ min}^{-1}$ from 380.0 K through melting to 628.0 K | 557.7 | |
| 1 | LST-1 | heated at $20^\circ \text{ min}^{-1}$ from 380.0 K through melting to 628.0 K | 555.2 | |
| 1 | LNC-1 | heated at $20^\circ \text{ min}^{-1}$ from 380.0 K through melting to 628.0 K | 485.2 | |
| 2 | LM-2 | cooled LM-1 rapidly and heated again at $20^\circ \text{ min}^{-1}$ from 380.0 K through T_g to 628.0 K | 501.2 (T_g) | no fusion observed |
| 2 | LM-3 | cooled LM-2 rapidly and heated again at $20^\circ \text{ min}^{-1}$ from 380.0 K through T_g to 628.0 K | 527.2(T_g) | no fusion observed |
| 3 | LM-4 | heated at 5° min^{-1} from 380.0 K through melting to 628.0 K | 552.5 614.1 | dual endotherms |

Figure 1. It was obtained at $20^\circ \text{ min}^{-1}$ and shows only one endotherm. At a slower scan rate, 5° min^{-1} , the endotherm is substantially diminished in area, and shifted to a slightly lower temperature, and a new endotherm appears at 614.1 K. The cumulative energies of transition measured in both thermograms are essentially equal. The diminution of the low temperature endotherm and its shift to a lower temperature at the lower heating rate must be attributed to an exothermic process concomitant with the endothermic process, yet lagging behind it slightly. The exothermic process, no doubt, is that which establishes the new more stable population of crystallites. Apparently the lower heating rate allows time for the annealing to take place to an appreciable extent.

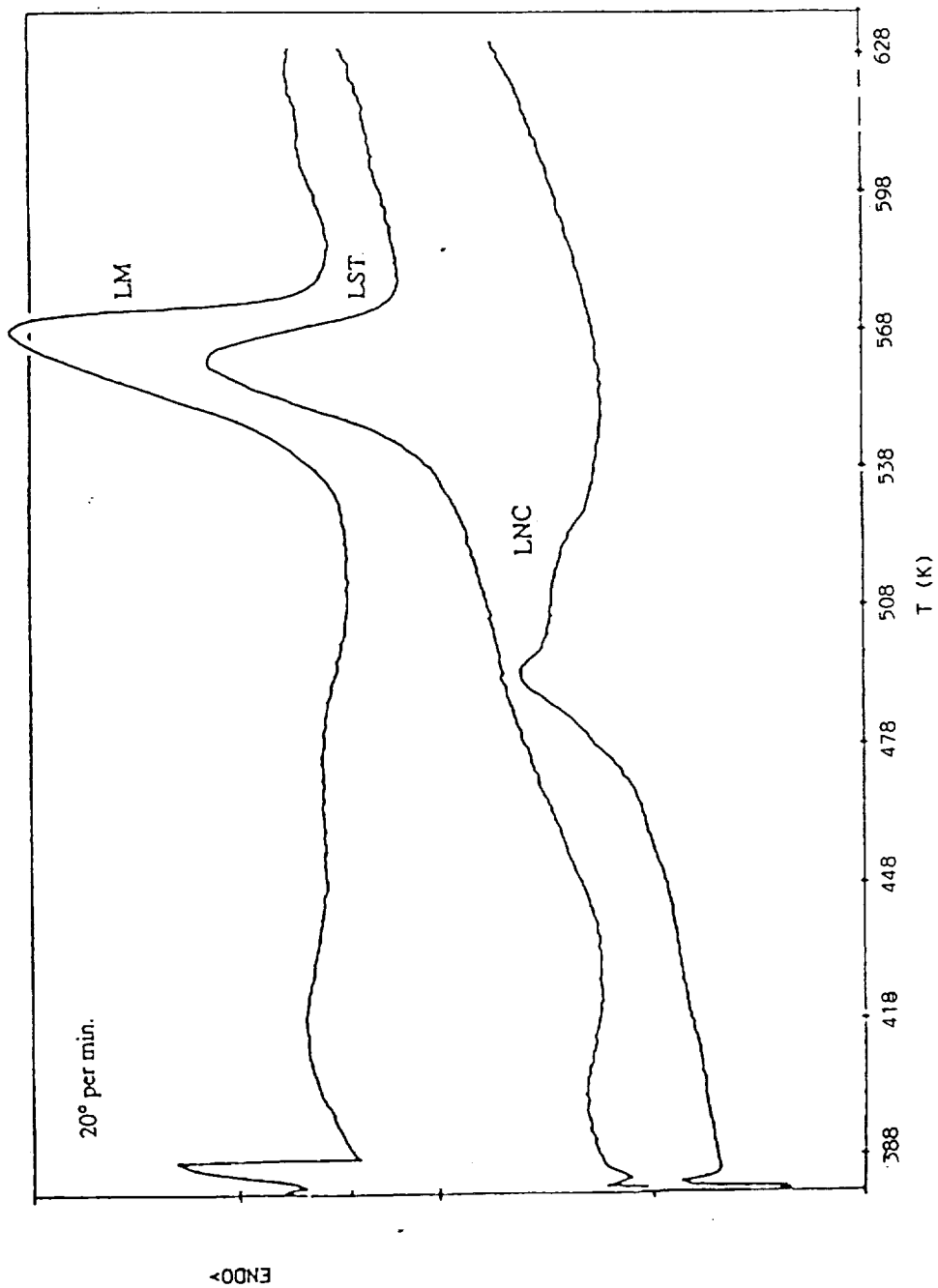


Fig. 1 Dsc heating thermograms for untreated LNC, LST, and LM samples.

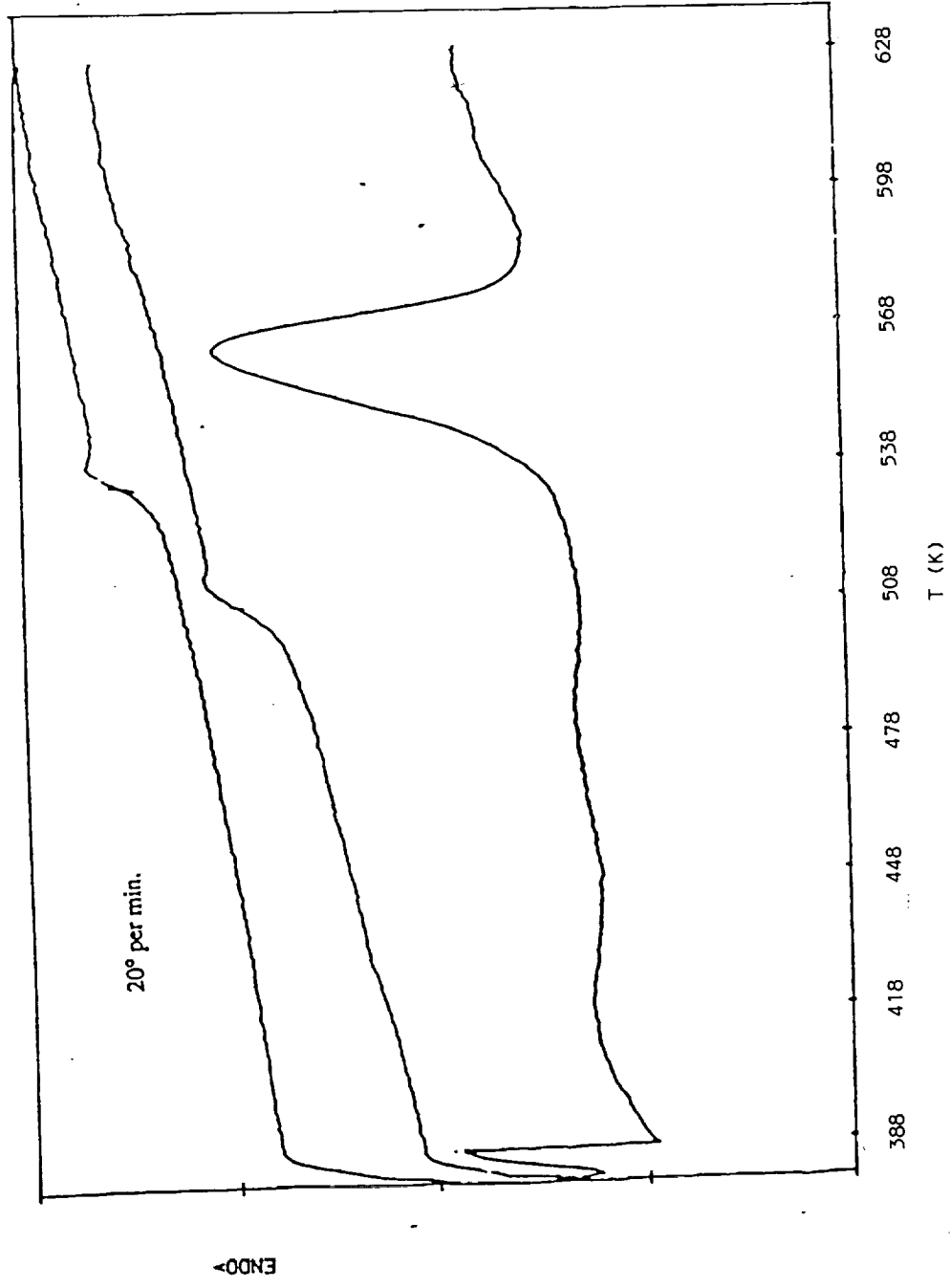


Fig. 2 Dsc heating thermograms of LM run in sequence from the bottom to the top of the figure.

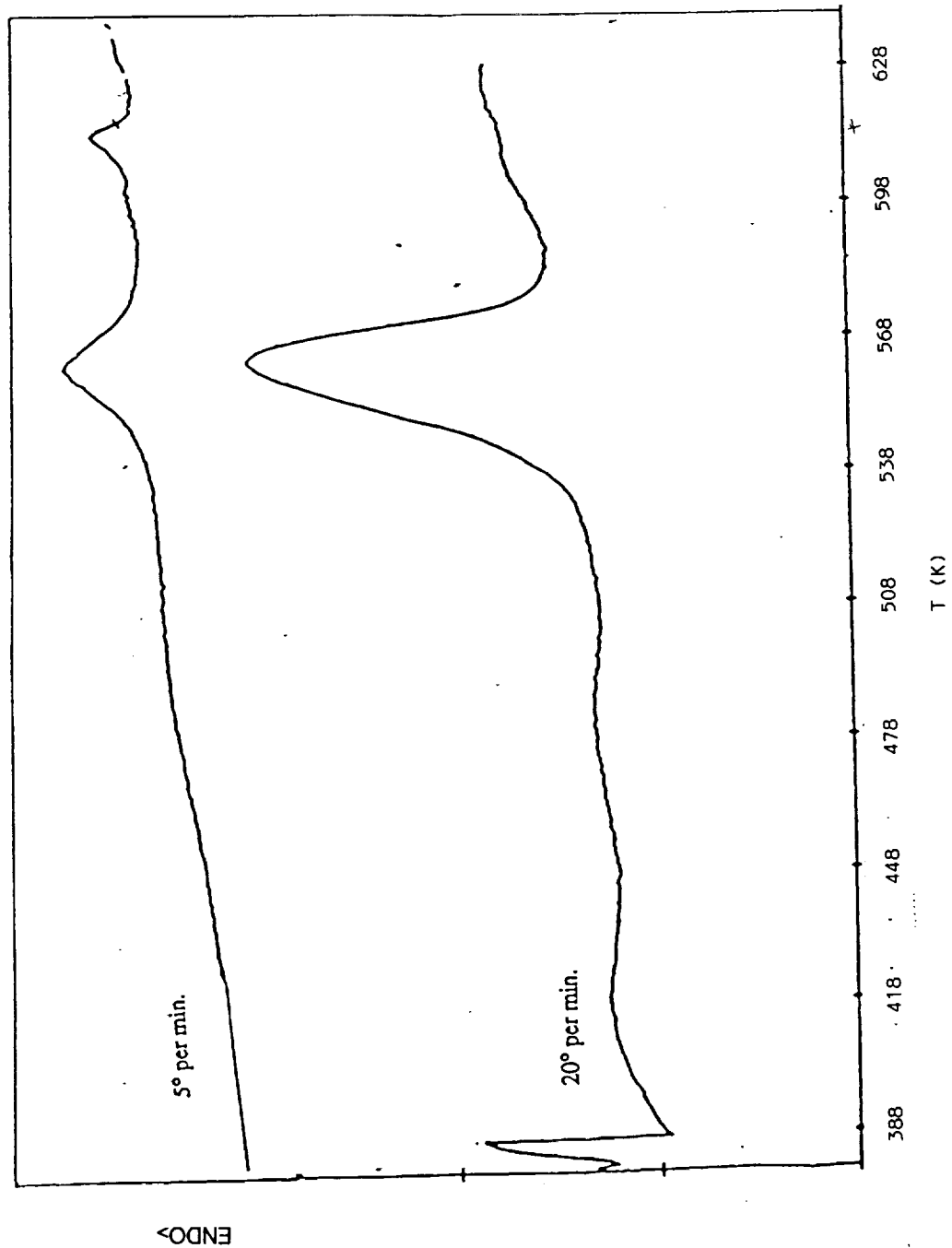


Fig. 3 Dsc heating thermograms of LM scanned at $5^{\circ} \text{ min}^{-1}$ and $20^{\circ} \text{ min}^{-1}$.

III.4 Annealing experiments involving LM

Table III.4 summarizes the trend seen in terms of melting temperatures and

TABLE III.4 Overall trends for annealing experiments on LM based on data given in Tables III.5-III.9.

Annealing conditions:

Isothermal holding time (min): 0, 5, 15, 30

Heating rate: 5 K min⁻¹

Holding temperatures (K): 400, 475, 525, 553, 575

Temperature range (K): 323 to 630

*

| Refer to Tables: | Annealing time (min) | Comments | | | |
|------------------|----------------------|----------------|-----------|--------------|--------------|
| | | $T_{m,1}$ | $T_{m,2}$ | ΔH_1 | ΔH_2 |
| III.5, III.9 | 0 | increase | no trend | decrease | decrease |
| III.6, III.9 | 5 | small increase | no trend | decrease | increase |
| III.7, III.9 | 15 | increase | no trend | decrease | increase |
| III.8, III.9 | 30 | increase | no trend | decrease | increase |

heats of fusion obtained after annealing the polymer at various temperatures with different holding times. It qualitatively summarizes the results of Tables III.5--III.8. Each of those tables, in turn, lists the first and second

Table III.5 Annealing of LM for 0 min

| Temperature (K) | $T_{m,1}$ (K) | $T_{m,2}$ (K) | ΔH_1 (J/g) | ΔH_2 (J/g) |
|-----------------|---------------|---------------|--------------------|--------------------|
| 400 | 552.2 | 612.1 | 32.60 | 6.82 |
| 475 | 552.6 | 612.2 | 28.41 | 2.76 |
| 525 | 552.0 | 612.2 | 37.66 | 6.07 |
| 553 | 556.6 | 610.9 | 21.72 | 19.50 |

Table III.6 Annealing of LM for 5 min

| Temperature (K) | $T_{m,1}$ (K) | $T_{m,2}$ (K) | ΔH_1 (J/g) | ΔH_2 (J/g) |
|-----------------|---------------|---------------|--------------------|--------------------|
| 400 | 552.2 | 613.2 | 44.18 | 7.66 |
| 475 | 554.5 | 613.6 | 27.78 | 8.08 |
| 525 | 553.8 | 614.7 | 32.09 | 8.45 |
| 553 | 560.0 | 610.6 | 13.47 | 24.85 |

Table III.7 Annealing of LM for 15 min

| Temperature (K) | $T_{m,1}$ (K) | $T_{m,2}$ (K) | ΔH_1 (J/g) | ΔH_2 (J/g) |
|-----------------|---------------|---------------|--------------------|--------------------|
| 400 | 552.6 | 612.7 | 31.46 | 8.20 |
| 475 | 552.2 | 612.9 | 28.54 | 5.69 |
| 525 | 552.8 | 612.0 | 31.00 | 8.54 |
| 553 | 563.6 | 615.8 | 20.67 | 22.13 |

Table III.8 Annealing of LM for 30 min

| Temperature (K) | $T_{m,1}$ (K) | $T_{m,2}$ (K) | ΔH_1 (J/g) | ΔH_2 (J/g) |
|-----------------|---------------|---------------|--------------------|--------------------|
| 400 | 552.7 | 612.8 | 29.12 | 6.03 |
| 475 | 553.3 | 612.8 | 32.22 | 6.11 |
| 525 | 553.2 | 613.0 | 26.07 | 5.65 |
| 553 | 562.1 | 613.0 | 11.72 | 23.81 |

melting temperatures observed and the respective experimental enthalpies of fusion, ΔH_1 and ΔH_2 , for a given annealing period at each annealing temperature. The initial melting temperature $T_{m,1}$ changes very little as annealing progresses through its lower temperature ranges. When annealing reached the vicinity of $T_{m,1}$ for the previously unannealed polymer, 553 K, we saw an increase in $T_{m,1}$ to ca. 562 K (Figure 4). The sample that was annealed for 0 min at 553 K shows a significant although smaller increase in $T_{m,1}$ than did those annealed for other durations. We may attribute this effect to the fact that this sample was cycled to 553 K, but not held there. Some annealing evidently occurred during that cycling process. However, we observed no trend with respect to the second melting temperature. As annealing temperature is increased for each annealing time, the enthalpy of fusion corresponding to $T_{m,1}$ tends to go down (Figure 5), while the enthalpy of fusion associated with $T_{m,2}$ tends to increase (Figure 6).

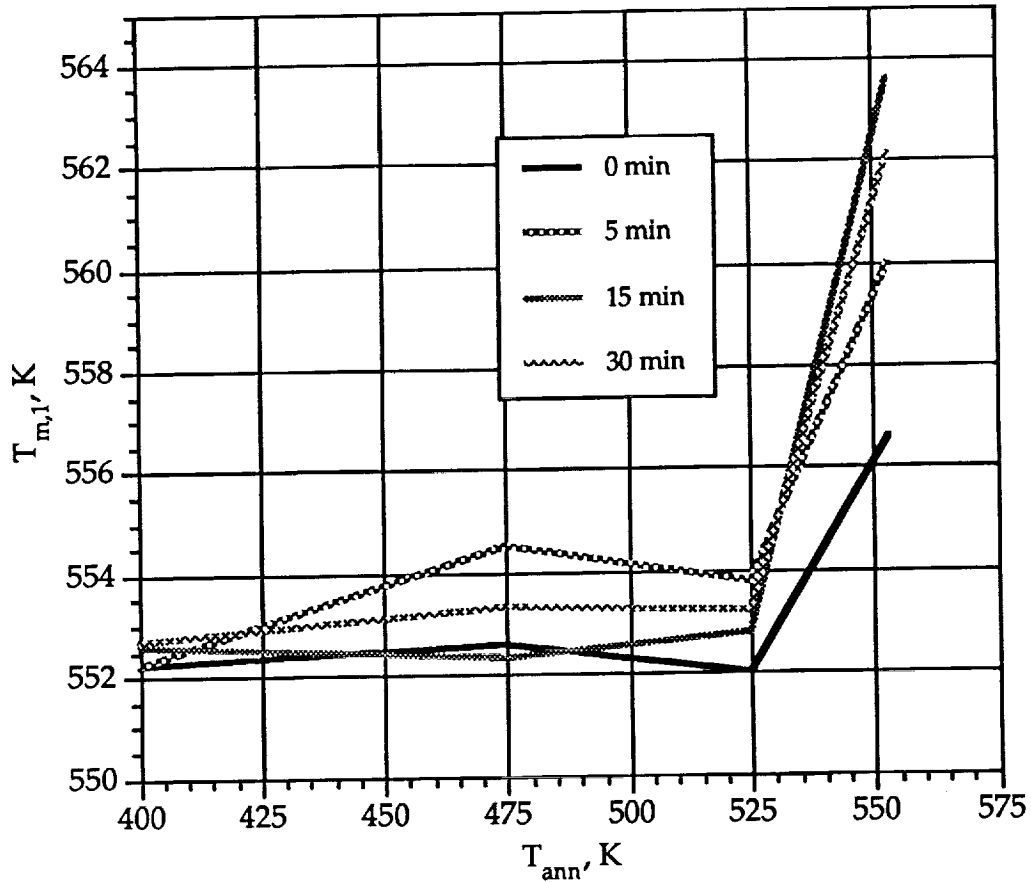


Fig. 4 Observed first melting temperature for LM vs. annealing temperature at the annealing times indicated in the legend.

The trend is somewhat weak and inconsistent for the lower annealing temperatures, but it is more pronounced at the higher annealing temperature. The trend for the enthalpy of fusion associated with $T_{m,2}$ is the inverse of the former one. Thus, annealing causes a portion of a phase that would melt at $T_{m,1}$ to be transformed to a more stable phase. Whether the transition occurs by a solid to solid route or through the melting of solid 1 followed by recrystallization to solid 2 is not definitively answered here. However, we do note that the transition process is time dependent as indicated by these experiments, and it occurs over a range of temperatures. It does not display the classical characteristic of inverse temperature dependence on rate that is characteristic of nucleation control. We can assume that the formation of solid 2 is nucleation dependent, but it seems to depend foremost on the disappearance of solid 1. In view of the yield increase of solid 2, when annealing takes place in the vicinity of $T_{m,1}$, the second mechanism, which involves the formation of an intermediate molten state, appears to be the more likely one.

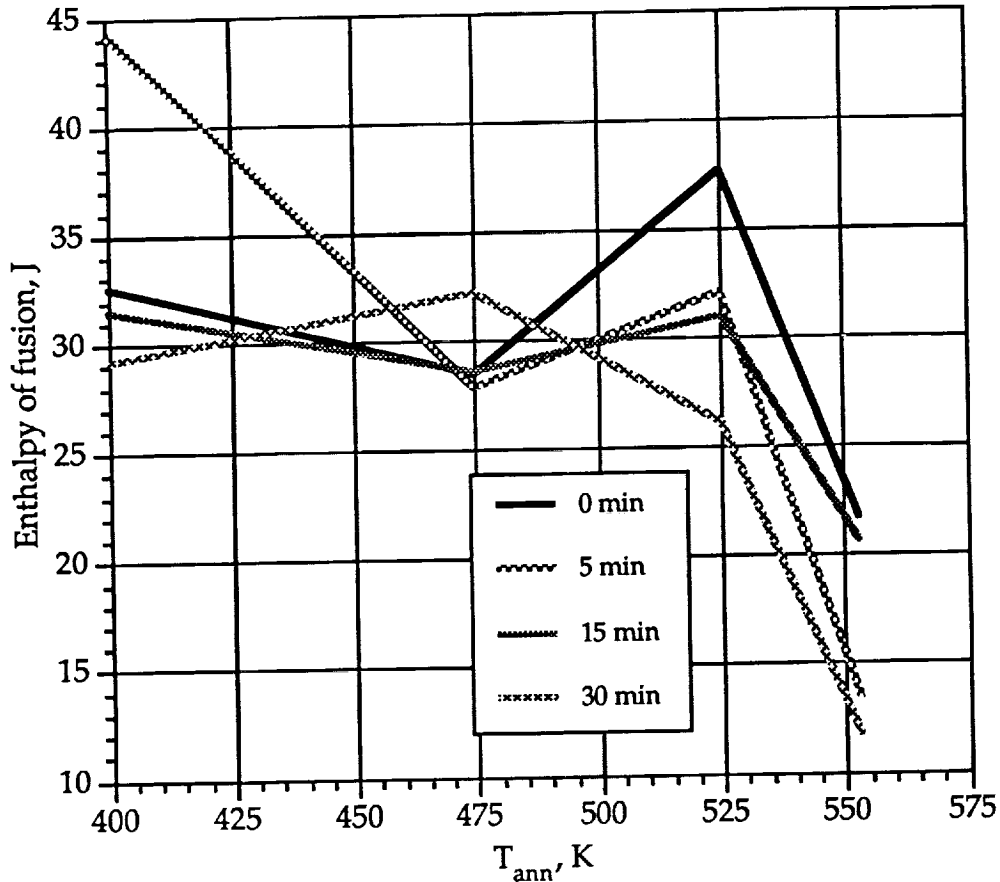


Fig. 5 Effect of annealing temperature upon enthalpy of fusion associated with $T_{m,1}$. Annealing times are indicated in the legend.

The LM sample was also heated to 575 K, beyond any $T_{m,1}$ that we had observed, and held there for durations that corresponded to those of Tables III.5 through III.8, *i.e.*, 0 min, 5 min, 15 min and 30 min. Because the isothermal hold temperature is beyond the $T_{m,1}$, we prefer to categorize these annealing experiments separately from the others. The results of these experiments are listed in Table III.9. The blank spaces in the table indicate that no melting at $T_{m,1}$

Table III.9 Annealing of LM at 575 K

| Time of annealing (min) | $T_{m,1}$ (K) | $T_{m,2}$ (K) | ΔH_1 (J/g) | ΔH_2 (J/g) |
|-------------------------|---------------|---------------|--------------------|--------------------|
| 0 | 557.3 | 612.0 | 3.97 | 19.92 |
| 5 | 551.6 | 612.0 | 3.51 | 22.59 |
| 15 | --- | 611.4 | --- | 27.20 |
| 30 | --- | 612.7 | --- | 28.74 |

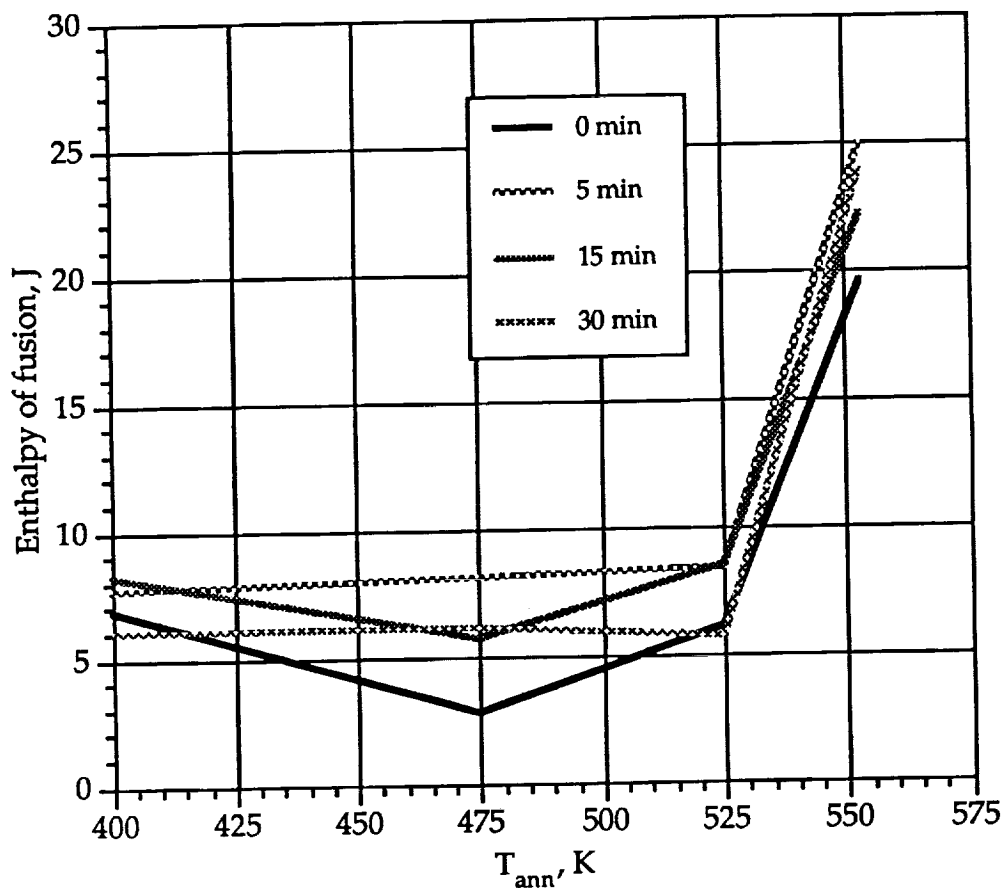


Fig. 6 Effect of annealing temperature upon enthalpy of fusion associated with $T_{m,2}$. Annealing times are indicated in the legend.

was observed for these longer annealing temperatures. Apparently with these longer annealing durations above $T_{m,1}$, the last vestiges of crystallinity that would melt at $T_{m,1}$ have been converted to more stable crystallites melting at $T_{m,2}$. That this conversion does take place is supported by the concomitant decrease in ΔH_1 and increase in ΔH_2 as the annealing time becomes longer. It is somewhat surprising that any crystallites that melt in the vicinity of 551-562 K remain after heating the sample to 575 K. Rather, it may be that after the shorter annealing periods of 0 min and 5 min, some heterogeneous nucleation on residues of the less stable crystallites takes place when cooling the samples prior to the melting experiments. At the longer annealing times, conversion to more stable crystallites is complete, and none of the less stable crystals remain or reform upon cooling.

III.5 Crystallization kinetics

Crystallization kinetics experiments were conducted at the temperatures indicated in Table III.10 on LM and LST. The temperatures chosen, 558.2 K to

Table III.10 Crystallization parameters for LM and LST in which the temperature of annealing was approached at $5^{\circ} \text{ min}^{-1}$

| Annealing temperature (K) | ΔH_{σ} (J/g) | | t_{max} (min) | | n | |
|---------------------------|---------------------------|--------|-----------------|-------|-------------|-----|
| | LM | LST | LM | LST | LM | LST |
| 558.2 | -45.30 | -10.04 | 10.32 | 10.82 | 1.6 | 1.4 |
| 562.2 | -51.52 -21.67* | -29.93 | 11.05 10.75* | 4.57 | 1.8 1.7* | 1.5 |
| 568.2 | -51.70 -33.03* | -13.65 | 10.53 9.60* | 12.81 | 2.1 2.0* | 1.7 |
| 572.2 | -35.73 | | 8.77 | | 2.0 | |
| 573.2 | -30.16 -15.62* | | 6.91 8.63* | | 2.1 1.8* | |

* Asterisks indicate starting times t_1 selected for analysis of data of 0.823 min after isothermal conditions were reached by the instrument; the absence of asterisks indicate t_1 of 0.85 min. Please see the text for a fuller explanation.

573.2 K inclusive, were in a range in which annealing experiments (Tables III.5-III.9) led us to believe that significant changes in the crystallinity of the polymers would take place. For the analysis of data, the starting time for the transition t_i was selected as 0.85 min after the instrument was brought to the annealing temperature by the instrument control program for those annealing experiment results not marked with an asterisk and 0.823 min for those results so marked. From our cumulative experience we were confident that the instrument sample holder had achieved thermal equilibrium, so the selection of t_i was consistent from one trial to the next. The selected t_i usually led to flat baselines when applying the software supplier's integration program to the crystallization exotherms. Events that happen in the early stages of a polymer crystallization take place in a less complicated system than those occurring in the advanced stages. For determination of crystallization mechanisms, use of early stage data is preferable. Data for analysis were always sampled within the first 28.2% of the extent of the transformation; for some annealing experiments, data were not sampled after 15.3% of the transformation. The heat of crystallization found per gram of polymer ΔH_{σ} was usually substantially higher for LM as compared to LST, thus demonstrating that the annealing process gives LM the higher yield of solid 2. With that exception there is reasonable quantitative agreement between the two polymers with respect to their annealing processes' kinetic parameters. The term t_{max} is the time required for the crystallization to reach its maximum rate. It is related to the rate constant k for crystallization by²¹

$$t_{max} = \left[\frac{-\ln\left(1 - \frac{X_c(t_{max})}{X_c(\infty)}\right)}{\frac{1}{X_c(\infty)}k} \right]^{1/n} \quad (3)$$

in which $X_c(t_{max})$ is the mass fraction of material that has crystallized at time t_{max} , $X_c(\infty)$ is the limiting mass fraction that has crystallized, and n is the Avrami exponent for the crystallization. The term $X_c(\infty)$ is included because polymer crystallizations generally do not involve total conversion of all amorphous polymer to crystalline material. Let $k' = (1/X_c(\infty))k$ and let $c_{max} = X_c(t_{max})/X_c(\infty)$. Then

$$\ln[-\ln(1 - c_{max})] = \ln k' + n \ln t_{max} \quad (4)$$

Thus, an increase in t_{max} would be reflected in a lower value for k' if the potential fractional conversion to crystalline material c_{max} remains constant and the mechanism remains unchanged as reflected in the value of n . Table III.10 shows that the values of n do change somewhat. They appear to increase with crystallization temperature. If n were constant, then the isotherms would be superposable²¹ and relative values of t_{max} would be interpretable in rankings of k and k' as suggested by equations 3 and 4. Leaving the results expressed in terms of t_{max} allows one to readily see which process is going to completion most quickly rather than being concerned with the less practical albeit theoretically important rate constants. Typical data plotted according to equation 4 to yield n and k' are shown in Figure 7. The correlation coefficient for this plot of data obtained at 573.2 K after approaching that temperature at 5° min^{-1} is 0.999. A value for n of 2.13 and a value of k' of $6.32 \times 10^{-3} \text{ min}^{-2.13}$ were obtained from this plot.

Often, a negative temperature coefficient for a phase transition rate is cited as evidence for a nucleation controlled process. Table III.10 shows a concomitant increase in n with a decrease in t_{max} . This combination unambiguously shows

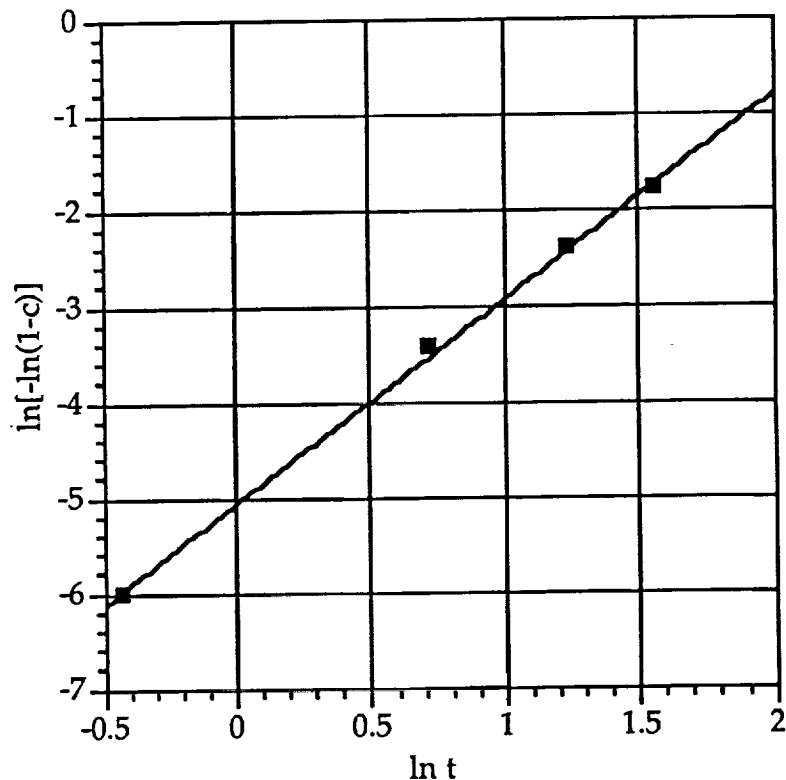


Fig. 7 Plot as suggested by equation 4 to determine K and n for an LM sample that was crystallized at 573.2 K after heating it to that temperature at 5° min^{-1} .

that the crystallization rate increases with temperature. The annealing temperatures of these experiments, from 558.2 K to 573.2 K are not far above T_g values observed for this polymer, 501.2 K and 527.2 K (Table III.3). Ultimately, the $T_{m(\text{obs})}$ for polymers so annealed are in the vicinity of 614 K. From this we may conjecture that the crystallizations were conducted below T_{max} , the temperature at which the crystallization rate would be a maximum. Hence, the positive temperature coefficient of the crystallization rate does not contradict the possibility of a nucleation controlled annealing process.

If the crystallization is nucleation controlled, we may then interpret the values obtained for n in that context. These values are higher than those obtained by Hou *et al.*²³ who conducted their annealing experiments from 553.2 K to 593.2 K. We should remark that the value of n determined is very sensitive to what one selects as the properties of the totally untransformed polymer, whether that property be specific volume, heat content or some other indicator of crystallinity. Our crystallizations detectably began as soon as the DSC sample holder reached thermal equilibrium, perhaps sooner. If we or Hou *et al.* chose the wrong starting times for the crystallizations, then those results would be somewhat in error. Nevertheless, we can say that Avrami exponents in the vicinity of 1.0 as found by Hou *et al.*²³ or between 1.4 and 2.1 inclusive as found by us, suggest a very low dimensional order to the nucleation process, combined with the possibility of

heterogeneous nucleation starting at the beginning of the process rather than randomly with time.

Since changing the heating rate applied to a sample from 5° min^{-1} to $20^\circ \text{ min}^{-1}$ had significant effects on the endothermic transitions of LM (Table III.3), we wished to see if the crystallization kinetics were significantly affected when the temperature of crystallization was approached by raising the temperature at 5° min^{-1} vs. $20^\circ \text{ min}^{-1}$. The comparison shown in Table III.11 includes data

Table III.11 Comparison of crystallizations for LM for annealing temperatures approached at 5° min^{-1} vs. $20^\circ \text{ min}^{-1}$ *

| Annealing temperature (K) | ΔH_c (J/g) | | t_{max} (min) | | n | |
|---------------------------|--------------------|---------|-----------------|-------|-------------|-------|
| | LM-5 | LM-20 | LM-5 | LM-20 | LM-5 | LM-20 |
| 558.2 | -45.30 | -50.26 | 10.32 | 16.69 | 1.6 | 1.5 |
| 562.2 | -51.52 -21.67* | | 11.05 10.75* | | 1.8 1.7* | |
| 568.2 | -51.70 -33.03* | -113.42 | 10.53 9.60* | 13.05 | 2.1 2.0* | 1.2 |
| 572.2 | -35.73 | | 8.77 | | 2.0 | |
| 573.2 | -30.16 -15.62* | -87.02 | 6.91 8.63* | 12.40 | 2.1 1.8* | 1.1 |

* Asterisks indicate starting times t_i selected for analysis of data of 0.823 min after isothermal conditions were reached by the instrument; the absence of asterisks indicate t_i of 0.85 min. Please see the text for a fuller explanation.

already given in Table III.10. The results of these annealing or crystallization kinetics experiments show that, in general, heating to the isothermal study temperature at $20^\circ \text{ min}^{-1}$ (LM-20) rather than 5° min^{-1} (LM-5) results in a more substantial exothermic transition during the isothermal holding period as shown in the second and third columns of Table III.11. When the isothermal study temperatures were reached at heating rates of $20^\circ \text{ min}^{-1}$, it was apparent from the melting continued for the less stable population of crystallites (section III.4). This phenomenon was particularly evident at the highest isothermal study temperature, 573.2 K. Therefore, in analyzing the rate data for these trials, we had no recourse but to select arbitrary t_i that differed among the trials in this group. For example, for the isothermal study temperature of 558.2 K, a t_i of 0.853 min was used, a value essentially the same as that used for the LM-5 series. However, for the study temperature of 573.2 K, t_i of 3.250 min had to be used. We present these results with the caveat that the inconsistencies with which we selected t_i should lead to some inconsistencies in the parameters obtained from our analysis of the kinetics data.

The difference between the LM-5 series and the LM-20 series with respect to the exothermic heat of transition is large and appears to be significant. The LM-20 series gives up more enthalpy per gram of polymer than the LM-5 series at each study temperature where comparison can be made. This result is puzzling since, as stated in section III.3, polymers heated at $20^\circ \text{ min}^{-1}$ show no

second exotherm in the vicinity of 614 K, while those heated at $5^{\circ} \text{ min}^{-1}$ yield a more stable population of crystallites. Apparently, it is the combination of the difference in heating rates and the isothermal holding period that causes these results to differ from those reported in section III.3. The t_{max} values show that the isothermal crystallization of LM-20 proceeds more slowly than that of LM-5. It is likely that for a continuous heating process with no isothermal pause at $20^{\circ} \text{ min}^{-1}$, LM has no chance to recrystallize, but at the slower heating rate it does. Thus this data supports the statement made at the end of section III.3.

In Table III.11 we see a difference obtained for the n values from one heating protocol versus the other. While these values are close to those obtained by Hou and Bai,²³ it is not clear that these differences from our other data are real or if they are apparent ones due to the experimental difficulties mentioned above.

III.6 X-ray diffraction

All three samples of LARC-TPI polymer powder in virgin form and the LM and LST samples after heat treatment were subjected to X-ray diffraction in order to better understand the changes in crystallinity that we observed through Dsc. All three polymers studied were found to be crystalline in as received or as prepared form, and the LST and LM versions of LARC-TPI were also examined by X-ray diffraction after heat treatments at 568.2 K. The d spacings for the virgin polymers are given in Table III.12.

Table III.12 X-ray diffraction on untreated and annealed LARC-TPI samples

| Sample | Thermal history | d spacings (nm x 10^1) |
|--------|-------------------------------------------------|--------------------------------|
| LST | used as received | 4.9 |
| | | 4.1 |
| | | 3.4 |
| LNC | used as prepared | 3.8 |
| LM | used as received | 5.6 |
| | | 4.6 |
| | | 4.2 |
| | | 3.4 |
| LM | Heated at 568.2 K under N_2 for 5 min | 4.6 |
| LM | Heated at 568.2 K under N_2 for 15 min | 4.8 |
| | | 4.2 |
| LM | Heated at 568.2 K under N_2 for 60 min | 6.1 |
| | | 5.3 |
| | | 4.8 |
| | | 4.2 |
| | | 3.5 |

The virgin LNC proved to be only marginally crystalline, the other two samples were more so. Their powder patterns are shown in Figures 8-10.

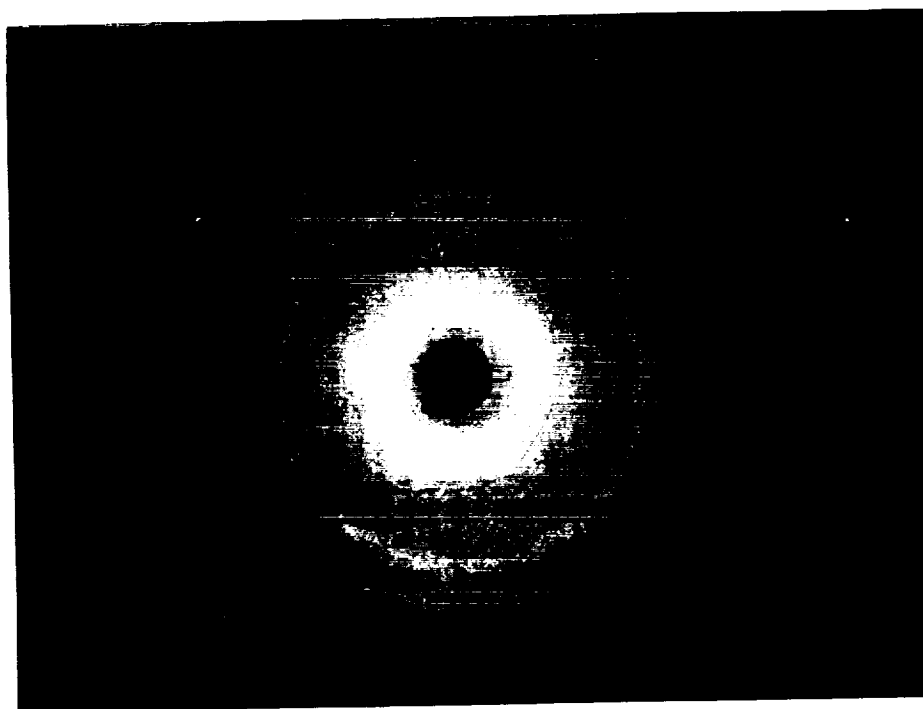


Fig. 8 X-ray diffraction powder pattern of virgin LST.

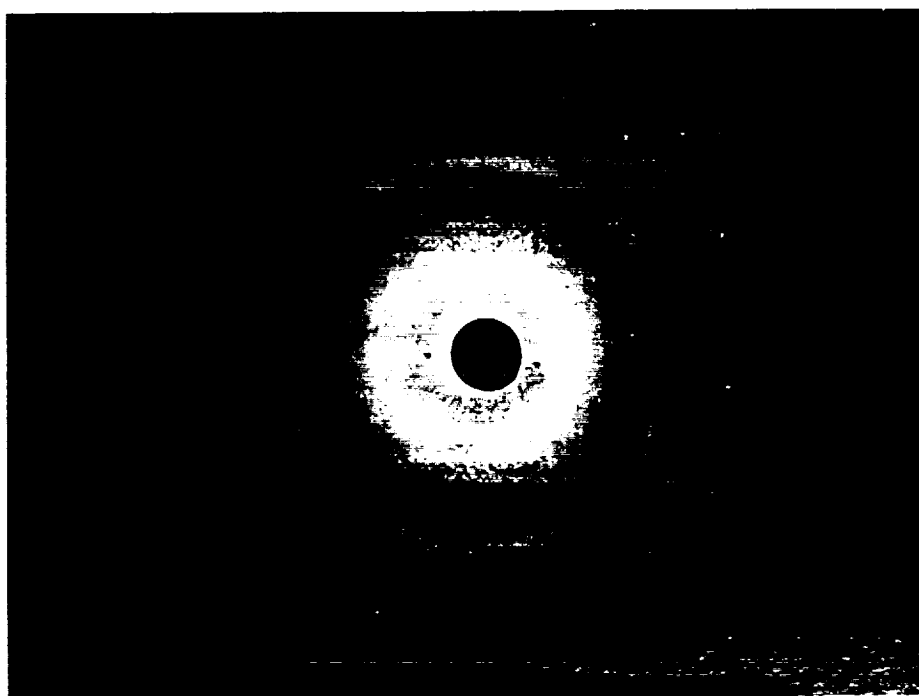


Fig. 9 X-ray diffraction powder pattern of virgin LNC.

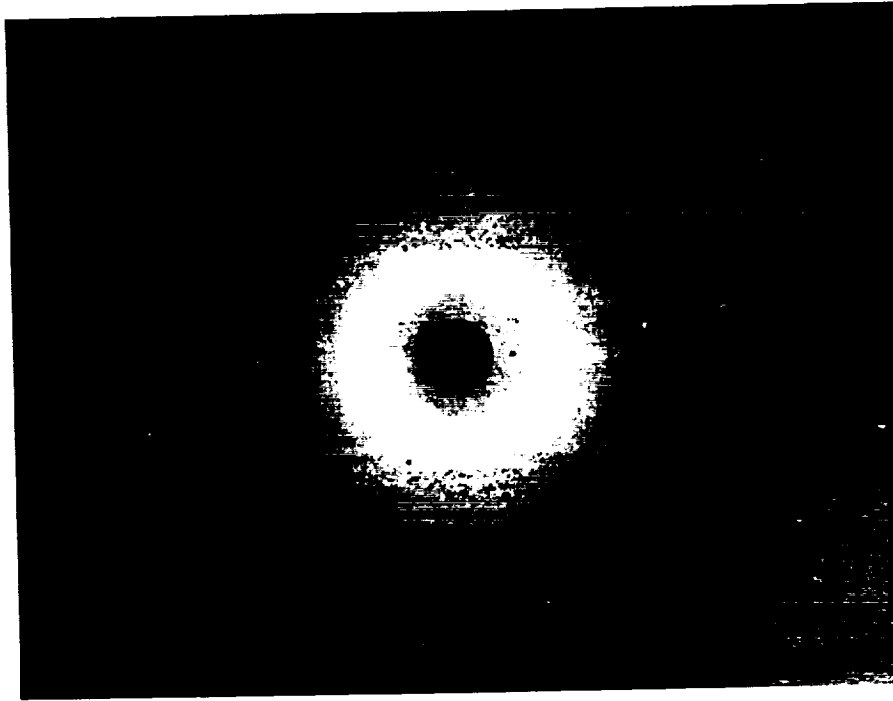


Fig. 10 X-ray diffraction powder pattern of virgin LM.

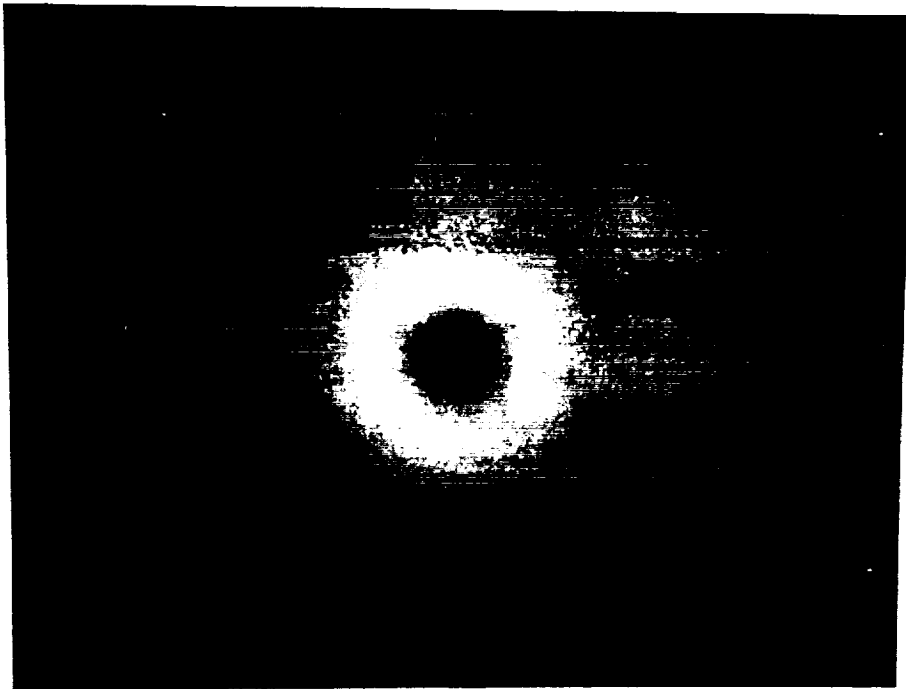


Fig. 11 X-ray diffraction powder pattern of LM annealed for 5.0 min at 568.2 K.

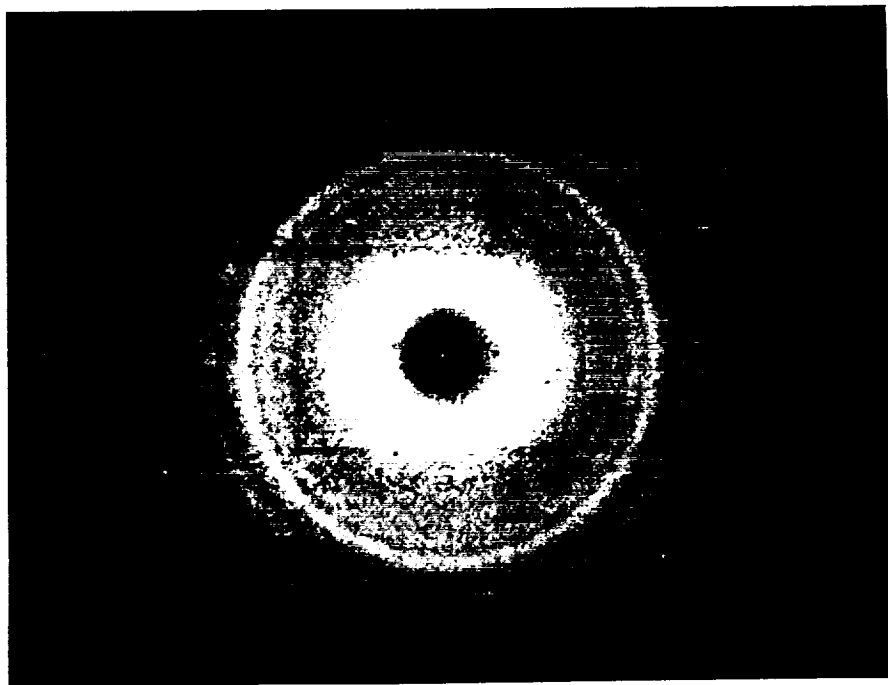


Fig. 12 X-ray diffraction powder pattern of LM annealed for 60.0 min at 568.2 K.

The diffraction patterns from the LST and LNC samples heated at 568.2 K did not show any evidence of crystallinity.

When heat treated at 568.2 K, the LM sample underwent a series of changes. The process appears to involve melting of the crystallites seen in the as received polymer followed by recrystallization. The crystalline diffraction rings seen in diffraction patterns of the untreated sample (Figure 10) fade after 5 min of annealing at 568.2 K (Figure 11). After continued annealing, a clearly defined new powder pattern emerges that is indicative of a new crystalline structure (Figure 12). The original crystalline structures of LM and LST were quite different as shown from the spacings of Table III.12. Examination of Table III.12 shows that as the annealing process continues, the new diffraction rings originating from the crystallites of LM are similar to those found in the untreated LST. Thus, annealing of LM has had the net effect of producing crystallites that have similar d spacings to virgin LST.

The disappearance of most of the crystallinity of LM after annealing at 568.2 K for 5 min, followed by the emergence of differently structured crystallites suggests that the transition of one crystalline form to another involved a molten intermediate. However, the fact that the LM cannot be recrystallized after melting the more stable solid 2, indicates that some remnants of the less thermally stable solid 1 serve as necessary nucleation sites for the transformation to the new crystalline structure.

III.7 Dissolution experiments

Hou and Bai reported that when LARC-TPI is completely melted it becomes amorphous and cannot be recrystallized. It then displays a glass transition upon heating as is characteristic of amorphous polymers. Subsequent cooling and reheating results in a higher T_g than previously observed.²³ In section III.3 we report confirmation of their results. It is reasonable to conjecture that the irreversibility of the crystallization process and the increases in T_g are caused by fundamental changes in the molecular structure of the polymer that occur upon heating. Hou and Bai proposed chain extension as one such possibility.^{14,23}

Since one of the structural units of polyimides is tetrafunctional, reaction to form crosslinked networks should also be considered. The presence of crosslinked structural units structures should inhibit crystallization. A sensitive test for crosslinking is probing for network formation by attempting dissolution of the polymer, since only a small degree of crosslinking will lead to the formation of insoluble networks.

Table III.13 gives the thermal history of the polymers to which we applied

Table III.13 Dissolution tests of LARC-TPI samples

| Sample | Thermal history | Sample Mass (kg x 10 ⁶) | Observation |
|--------|---------------------------------------------|----------------------------------------|-------------------|
| LM | used as received | 5.2 | dissolved |
| LST | used as received | 7.8 | dissolved |
| LNC | used as prepared | 3.4 | dissolved |
| LM | 303.2 K to 633.2 K at 5° min ⁻¹ | 2.4 | insoluble residue |
| LST | 303.2 K to 593.2 K at 20° min ⁻¹ | 8.7 | insoluble residue |
| LNC | 303.2 K to 543.2 K at 20° min ⁻¹ | 3.7 | insoluble residue |

the solubility tests described in section II.2.g as well as the results of the tests. The different heating protocols were conservative ones and reflect temperatures not very much in excess of that required to melt each sample completely. It is noteworthy that the untreated crystalline samples dissolved, while the amorphous heat treated ones did not. If the polymers were not crosslinked in both cases, the crystalline one would dissolve with more difficulty than the amorphous one, since its crystalline regions would have to acquire their enthalpies of fusion in addition to the enthalpies required for dissolution. Thus, it appears that the heat treatments did cause some network formation.

IV Summary and conclusions

The substance known as the polyimide LARC-TPI represents, in reality a class of polyimides that have structural differences among them, including degree of imidization. When we examined LARC-TPI samples of different origins, we found fundamental differences among them. From a chemical structure standpoint we found a difference in the potentials for further imidization among the samples that we have designated as LM, LST and LNC. Of the three, LM was the most unresponsive to heating conditions that would normally lead to further imidization. Thus we see gross differences in the chemical structures of these LARC-TPI samples. These chemical differences, together with others not examined here, lead to property differences among them. This study dealt with thermal properties or those induced by thermal treatments and emphasized the polymer designated as LM.

We found that when the virgin polymers were heated at a rate that did not allow for detectable annealing, LM, showed the highest crystalline melting temperature of the three. Once completely melted, LM did not recrystallize upon cooling. Rather, it displayed a glass transition which in turn rose to a higher value on a subsequent cooling and reheating cycle. The LARC-TPI samples proved to be soluble in *m*-cresol in their virgin states. However, when each polymer was heated beyond their observed melting temperatures and cooled, the polymers were no longer totally soluble. Thus we are led to conclude that there is a strong possibility that crosslinking takes place in LARC-TPI once it is heated beyond $T_{m(obs)}$. Consistent with our experimental experience, crosslinking, which is known to occur in polyimide systems,¹⁷ would tend to create an insoluble gel, inhibit recrystallization, and raise the T_g of an amorphous polymer.

Annealing experiments, either conducted isothermally or by slow heating, results in the formation of a new more stable population of crystallites that melts *ca.* 45 °K higher than the crystallites found in the virgin polymer. X-ray diffraction shows that the initially present crystalline phase to nearly vanishes before the second phase is manifested, indicating that the transition to the new crystalline phase involves a solid-liquid-solid transformation. The fact that the annealing process takes place in the vicinity of the melting temperatures of the less thermally stable population of crystallites suggests that the remnants of these mostly molten crystallites are required for further crystallization to occur.

The temperature coefficient of the annealing process is positive over the temperature range studied. However the crystallization isotherms observed are characteristic of a nucleation controlled process. Crystallization kinetics studies of this transformation yield Avrami exponents of 1.4-2.1 when LM and LST are heated to the isothermal study temperature at 5° min⁻¹ and, with some experimental uncertainty, Avrami exponents *n* of 1.1-1.5 are found for a 20° min⁻¹ initial heating rate. These low Avrami exponents suggest that the nucleation process is of a low spatial dimensional order. Furthermore, it would appear to be heterogeneous with all embryonic nuclei forming at the beginning of the crystallization. We further believe that from the positive temperature coefficient observed for the process that diffusion controlled rates may also be affecting the value of the observed Avrami exponents.

Therefore, the properties of LARC-TPI can be very strongly dependent on how it was synthesized and upon subsequent thermal treatments applied to this polyimide.

V REFERENCES

1. Kirk-Othmer "Encyclopedia of Chemical Technology", 18, 3rd ed., J. Wiley and Sons, New York, 1978, Vol. 18, p. 704.
2. M. T. Bogert and R. R. Renshaw, *J. Am. Chem. Soc.* **30**, 1135 (1908), C.A. 2, 2681 (1908).
3. U. S. Pat. 2, 710, 853 (1955) [DuPont Company]; C. A. 50, 5753d (1956).
4. (a) W. M. Edwards, U.S. Pat. 3, 179, 614 (April 20, 1965);(b) U.S. Pat. 3, 179, 634(April 20, 1965); (c)British Pat. 898, 651(September 18, 1959).
5. (a) A. L. Endrey, U.S. Pat. 3, 179, 631(April 20, 1965); (b) U.S. Pat. 3, 179, 633(April 20, 1965); (c) Can. Pat. 659,328(March 12, 1963).
6. J. I. Jones, F. W. Ochynski and F. A. Rackley, *Chem. Ind.*, (London) 1686 (September 22, 1962).
7. C. E. Sroog, A. L. Endrey, S. V. Abramo, C. E. Berr, W. M. Edward and K. L. Olivier, *J. Polym. Sci, A*, **3**, 1373 (1965).
8. C. E. Sroog, *J. Polym. Sci. Part C, No. 16*, 1191 (1967).
9. G. M. Bower and L. W. Frost, *J. Polym. Sci., Polym. Chem. Ed.*, **14**, 2275 (1976).

10. M. I. Bessonov, M. M. Kotin, V. V. Kudryavtsev and L. A. Lavin, "Polyimides - Thermally Stable Polymers," Consultants Bureau, New York, 1987.
11. V. L. Bell, B. L. Stump, and H. Gager, *J. Polym. Sci., Polym. Chem. Ed.*, **14**, 2275 (1976).
12. D. J. Progar, V. L. Bell and T. L. St. Clair, U. S. Pat. 4,065, 345 (1977).
13. P. M. Hergenrother, *Chemtech*, **14**, 496, (1984).
14. T. L. St. Clair, NASA, Langley Research Center, personal communication 1987.
15. T. H. Johnston and C. A. Gaulin, *J. Macromol. Sci., Chem*, **A3 (6)**, 1161, (October 1969).
16. A. K. St. Clair and T. L. St. Clair, in "Polyimides, Synthesis, Characterization and Applications, Vol. 2", Ed. K. L. Mittal, Plenum press New York, 1984, p.977.
17. "Polyimides, Synthesis, Characterization and Applications, Vol. 1", Ed. K. L. Mittal, Plenum Press, New York, 1984.
18. A. K. St. Clair and T. L. St. Clair, *SAMPE Quarterly*, **14 (1)**, 20, (October 1981).
19. "Growth and Perfection of Crystals", R. H. Doremus, B. W. Roberts and D. Turnbull, John Wiley & Sons, Inc., New York, 1958.
20. A. Sharples, "Introduction to Polymer Crystallization", London, Edward Arnold, 1966.
21. L. Mandelkern, "Crystallization of Polymers", McGraw-Hill, New York, 1964,
22. M. H. Theil, *J. Polym. Sci., Polym. Phys. Ed.*, **13**, 1097 (1975).
23. (a) T. H. Hou, and J. M. Bai, submitted to Society of Plastics Engineers, ANTEC 87, Los Angeles, CA, April, 1987. (b) H. D. Burks, T. L. St. Clair and Tan-Hung Hou, *SAMPE Quarterly*, **18, 1**, (October 1986).
24. N. T. Wakelyn, NASA, Langley Research Center, personal communication, 1986.